CHAPTER 9

Advances in Oil/Water Separation of Biomimetic Superhydrophobic Coatings

ZHIGUANG GUO*[a,b] AND FUCHAO YANG[a,c]

[a] State Key Laboratory of Solid Lubrication, Lanzhou Institute of Chemical Physics, Chinese Academy of Sciences, Lanzhou 730000, People's Republic of China; [b] Hubei Collaborative Innovation Centre for Advanced Organic Chemical Materials and Ministry of Education Key Laboratory for the Green Preparation and Application of Functional Materials, Hubei University, Wuhan 430062, People's Republic of China; [c] University of Chinese Academy of Sciences, Beijing 100049, People's Republic of China
*Email: zguo@licp.cas.cn

9.1 Introduction

As a general consensus, environmental protection has long been a particularly important issue. Unfortunately, oil or organic chemical leaks during industrial accidents or oil tankers sinking happen frequently.[1] For example, oil spill accidents have continued to occur, from the 1967 Torrey Canyon oil spill to the latest 2011 Bohai Bay oil spill.[2] The explosion of the ''Deep water Horizon'' oil rig,[3] the most serious pollution incident of the last decade, is catastrophic for the environment and the effect is long term and lethal, especially for marine and aquatic ecosystems. It has also produced an abominable influence on people's normal life.[4] To address the oil spill, artificial separation, rather than burning, of the oily water is a more satisfactory way. Burning the as-spilled oil would waste energy and create

RSC Smart Materials No. 21
Self-cleaning Coatings: Structure, Fabrication and Application
Edited by Junhui He

Published by the Royal Society of Chemistry, www.rsc.org

more environmental pollution while the separation of as-spilled oil can be re-collected and reused in various industries. Aside from these, wastewater from industries such as petrochemicals, food, textiles, leather, and metal processing, has not been treated completely and discharged, resulting in lasting detrimental ecological effects. In order to deal with these issues, researchers have paid more and more attention to investigating separating oil/water mixtures.[5]

Until now, methods applied to separating oil/water mixtures have been gradually put forward.[6] Previously, some conventional techniques were employed to deal with oily wastewater, *i.e.*, centrifuges, oil skimmers, coalescers, settling tanks, gravity separations, ultrasonic separations, coagulation, an electric field, and flotation technologies.[7] During these separation processes, low separation efficiency, high energy consumption, and the secondary pollutants are limited to their wide applications. Thus, it is highly desirable to look for more efficient and economical methods to solve these problems.[5]

Essentially speaking, the oil/water separation is the wettability behavior that occurs at the interface of the solid, air, water and oil phase. Materials with superhydrophobic surfaces, one of the extreme states of surface wettability, have been inspired, intensively explored and accelerated by the discovery of a lotus leaf's self-cleaning phenomenon in nature.[8] Various porous or pulverous superhydrophobic materials have been investigated for the absorption and removal of various kinds of oils and organic solvents from oily wastewater. If the oil/water mixture is in an emulsified state, materials usually used for immiscible oil/water separation may be invalid because of the smaller droplet size. An elaborate membrane filtration technology was developed and can often be used to separate various emulsions.

In this chapter, we will begin with the understanding and design of the superhydrophobic surface, its definition, approaches to superhydrophobic surfaces and endowing some special materials with superhydrophobic property. Next, we will discuss various oil–water separations based on various superhydrophobic or superwettable materials. As for the separation of emulsified oil/water mixtures, the materials for the separation of water-in-oil, oil-in-water, and both water-in-oil and oil-in-water emulsions will be sequentially introduced. Followed by these, the principles to optimal design of materials bearing on separating oil–water mixtures are presented. Finally, the summary and outlook concerning future development of oil–water separations will be included.

9.2 Understanding and Design of the Superhydrophobic Surface

9.2.1 Understanding the Superhydrophobic Surface

It is widely accepted that wettability is the tendency of a liquid to spread on a solid substrate and is characterized by the water contact angle (WCA).

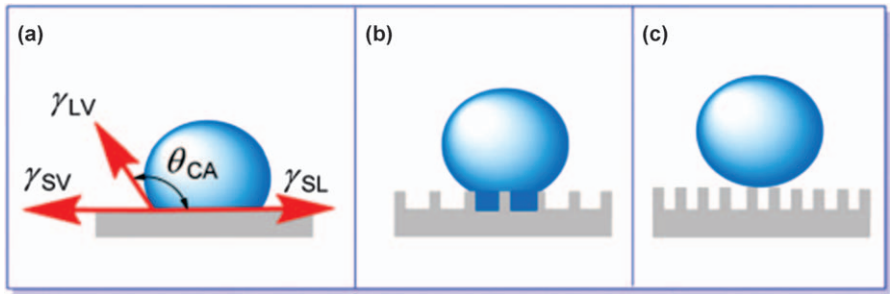

Figure 9.1 Schematic illustration of a droplet placed onto a flat substrate (a) and rough substrates (b) and (c). The droplet on a rough surface is either in a Wenzel state (b) or a Cassie–Baxter state (c).
Reproduced from ref. 11 with permission from the Royal Society of Chemistry.

The WCA is defined geometrically as the angle formed by a liquid droplet at the three phase boundary where a liquid, gas and solid intersect each other as shown in Figure 9.1(a).[9] The value of WCA on a surface can be used to determine the degree of affinity between liquid and solid, denoting a surface with contact angle (CA) below 90° as hydrophilic. If the CA value on a surface is larger than 90°, then it can be denoted as a hydrophobic surface.[10] The sliding angle (SA), is a threshold tilting value of the angle between the surface and horizon line, above which a liquid droplet starts to roll/slide upon elevating an end of the surface.[11] The SA of a water droplet on a solid surface is also an important parameter for predicting its wetting behavior in practical applications.[12] Generally, a superhydrophobic surface is defined as having a WCA greater than 150° but a SA less than 10° for a 5 μL droplet. Such surfaces commonly exist in the biological world and many plant leaves (lotus leaf,[9b] ramee rear surface[13]) and specific surfaces of animals (water striders,[14] eyes of mosquito[15]) in nature exhibit their superhydrophobic surface. As for a superhydrophobic surface, the interplay of surface microstructure and chemical composition causes water droplets to remain spherical on this kind of surface or slide away easily.

Next, we will discuss the effect of roughness factor and free surface energy on the wettability of solid surface. For an ideal smooth solid surface, Young's equation can be expressed as follows:

$$\cos\theta_0 = \frac{\gamma_{SA} - \gamma_{SL}}{\gamma_{LA}} \tag{9.1}$$

where γ_{SA} and γ_{LA} are the surface energies (surface tensions) of the solid and liquid against air, and γ_{SL} is the interface energy (interface tension) between solid and liquid. In a practical situation, the roughness of a solid surface can greatly magnify the wetting properties of this solid even without taking into

account any other potential influence factors. The ''roughness factor'' can be denoted by r and is given as:

$$r = \text{roughness factor} = \frac{\text{actual surface}}{\text{geometric surface}} \tag{9.2}$$

It should be pointed out that the area of the actual surface will be always greater than that of the geometric surface (the surface measured in the plane of the interface). Wenzel proposed an equation that gives a relation between the equilibrium CA and the apparent angle formed on a rough surface, referred to as the Wenzel equation:

$$\cos\theta_W = r\cos\theta_0 \tag{9.3}$$

where θ_0 is the equilibrium CA, θ_W is the apparent CA on a rough surface and the Wenzel state is schematically shown in Figure 9.1(b). This equation directly tells us that the roughness can amplify the wetting property of the solid surface. That is to say, if a water droplet is initially wetting on a smooth surface, the roughness would lead to greater hydrophilicity; if a water droplet is originally non-wetting on the smooth surface, then the introduction of the roughness can make the surface of the solid substrate even more non-wetting, resulting in an enhancement of hydrophobicity.

The Wenzel equation has revealed the apparent CA on a rough surface, but it would be invalid while the solid surface is porous or composed of diffident composition. Cassie and Baxter further amended the equations proposed by introducing the surface coefficient, referred to as the Cassie–Baxter equation given below:

$$\cos\theta_{CB} = f_{SL}(1 + \cos\theta_W) - 1 \tag{9.4}$$

where f_{SL} represents the solid–liquid fraction under the contact area and the Cassie–Baxter state is schematically shown in Figure 9.1(c). When $f_{SL} = 1$, the Cassie–Baxter equation turns into the Wenzel equation.

On the other hand, water droplets initially wetting or non-wetting an ideal smooth surface depends on its surface properties. Surface atoms or molecules of liquids or solids have higher energy than similar atoms and molecules in the interior, which results in surface tension or surface free energy (surface energy) so as to reach a stable state with a relatively lower energy. So the surface energy or surface tension can be used to evaluate the surface properties. In general, increasing the surface roughness was not directly based on a low-surface-energy substrate and then modifying the as-prepared rough surface with low-surface-energy materials is obligatory. Special low-surface-energy materials will be illustrated later in this chapter. This elucidation regarding roughness and surface properties is helpful for us to make surfaces with a superhydrophobic property.

9.2.2 Approaches to a Superhydrophobic Surface

Based on the preceding section, we bear in mind that the surface roughness and surface energy (chemical composition) are both crucial factors for the formation of superhydrophobic surfaces. Numerous fabrication methods have been developed for the preparation of rough surfaces, each having their own strengths and weaknesses.[16] They are often divided into two basic approaches: the top-down method and the bottom-up method.[17]

As for the top-down method, etching, lithography and anodization are widely used. Etching—removal of material from original surfaces—is a facile process to produce a rough structure and can be separated into wet etching and dry etching. Based on wet etching, Guo *et al.* have produced rough surfaces on aluminium and its alloy with binary structures at micro- and nanometer scales by subtle oxidation[18] and Zhang *et al.* prepared microflowers and nanorod array hierarchical structures on a copper substrate by immersing it into a mixed solution of NaOH and ammonium persulfate ($(NH_4)_2S_2O_8$).[19] Laser processing is an example of dry etching to construct a special surface topography. Yong *et al.* prepared spike-like structures on a flat Si surface *via* femtosecond laser micromachining by a line-by-line and serial scanning process, as shown in Figure 9.2.[20] Utilizing the technique of lithography, surfaces can be patterned with different shapes and different sizes. Jo *et al.* firstly prepared a ZnO nanoparticles dispersion resin and then patterned a circular cone-shaped micro-pattern with the as-prepared resin by ultraviolet nanoimprint lithography.[21] Anodization, often used as a material protection technology, is a kind of metal surface treatment in which the surfaces of a metal and its alloy form an oxide film through an impressed anodic current in an electrolyte solution. Barthwal *et al.* fabricated a rough surface based on a Ti plate *via* anodization.[22] The TiO_2 nanotube arrays are tightly formed on the entire surface of the Ti substrate with a satisfactory appearance.

As for the bottom-up methods, electrodeposition, the hydrothermal method and the sol–gel process are selected as representatives. Electrodeposition is aimed at covering the substrate with a layer of metal. The surface morphology can be controlled by changing monomer structures and the electrochemical parameters. We have fabricated rough copper mesh films *via* a facile and environmentally friendly method by electroplating Cu nanoparticles on as-cleaned copper mesh films.[23] The hydrothermal method, the products of which are high purity uniformly disperse, is another useful technique to create roughness. We have prepared a rough surface based on hierarchical rutile TiO_2 flowers through a simple one-step hydrothermal method.[24] The flower-like structure was made up of many petals on the surface obtained and each petal consisted of many ultrathin nanoneedles as shown in Figure 9.3 and these rough coatings show superamphiphilicity in air. As for the sol–gel process, chemical solution or sol is utilized as a precursor. When a large amount of solvent remains in the network during the network formation process, a gel is formed after a series

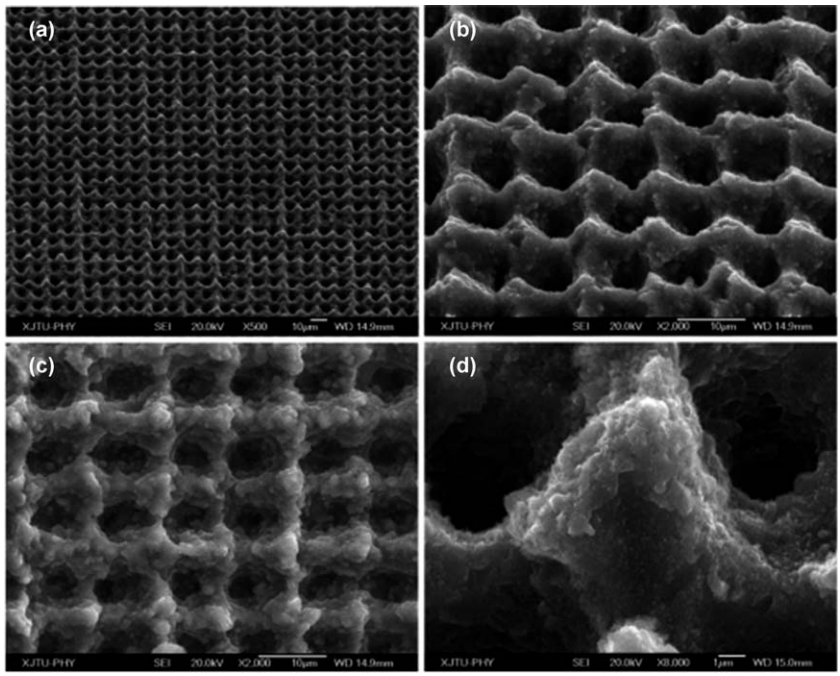

Figure 9.2 Typical SEM images of a structure irradiated by femtosecond laser. (a) 45° tilted view SEM image. (b) Higher resolution 45° tilted view SEM image. (c) Top view SEM image. (d) High magnification SEM image of a single spike decorated with nanoscale protrusions.
Reproduced from ref. 20 with permission from the Royal Society of Chemistry.

of hydrolyses of the precursor.[25] The sol–gel method can be applied to many kinds of substrates, such as metals, silicon wafers, glass, and textiles, fabricating superhydrophobic coatings.[26] We have developed a feasible method to fabricate a spray of sol–gel nanocoatings which can realize transparent superhydrophobic coatings on most solid surfaces through a mild process without any pre-treatment.[27]

We found that the top-down method achieves a surface topography with high control, and the bottom-up method usually leads to a random structure.[28] However, the top-down method is difficult to put into effect.

These methods are applied to construct a rough surface. Usually, surface modification with low surface energy materials is required for fabricating a superhydrophobic surface.[29] Until now, various kinds of low-surface-energy coatings have been developed as shown in Figure 9.4, such as, alkanethiols,[30] organic silanes,[31] fatty acids,[32] aromatic azide,[33] and fluorocarbon.[34] Alkanethiols are a kind of low-surface-energy materials bearing a hydrophobic alkyl chain and a thiol group as a surface anchor. Organic silane was used to modify surfaces bearing hydroxyl groups (hydrophobicity of its alkyl chain), such as silicon wafers, glass slides, silicon nanoparticles

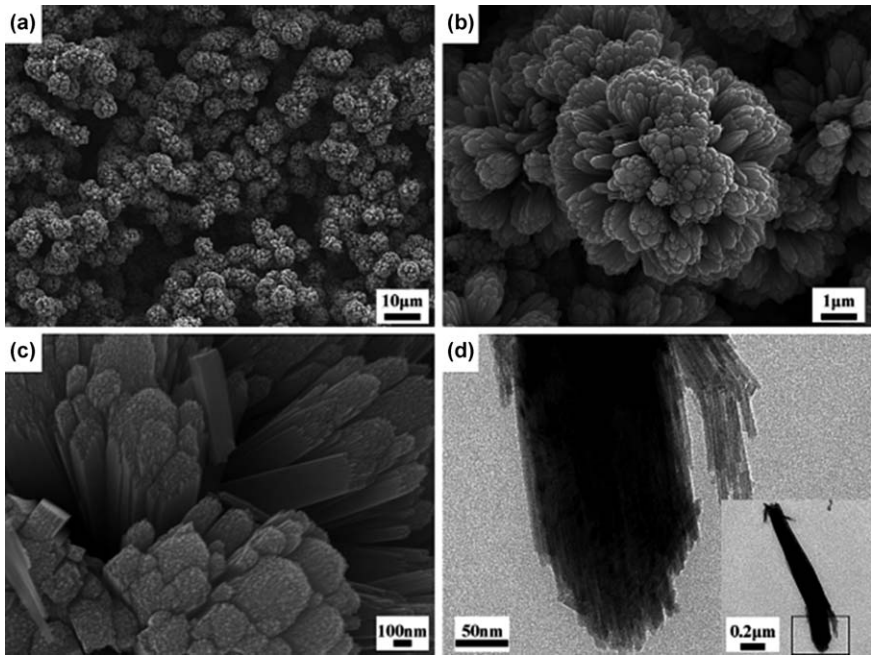

Figure 9.3 FE-SEM images of hierarchical rutile TiO_2 flowers: (a) top view of flower clusters, (b) top view of an individual flower, and (c) the close-up of nanopetals. (d) The close-up of a selected area enclosed by a black rectangle in inset; the inset shows TEM image of a single nanopetal.

and zeolite, to create low-surface-energy coatings.[31] Fatty acid is another important low-surface-energy material and surface wetting ability with different contact angles can be obtained by modifying rough surfaces with different lengths of alkyl chain. By use of a surface-reactive molecule of 4-azido-*N*-dodecylbenzamide with a molecule bearing an alkyl chain as a hydrophobic tail and an azide group as the reactive surface anchor, Zhang *et al.* developed a simple and convenient method to provide stable low-surface-energy coatings on organic surfaces.[33] The chemical composition determines the low surface free energy, and a lower surface energy leads to higher hydrophobicity.[35] Generally, these low-surface-energy coatings were usually anchored on the rough substrate by self-assembled or spin-coating methods. Self-assembled monolayers (SAMs) are molecular assemblies that are formed spontaneously by the immersion of an appropriate substrate into a solution of an active surfactant in an organic solvent.[29]

9.2.3 Endowing Special Materials with a Superhydrophobic Property

The special materials here have the potential to be used for oil–water separations. These functional materials mainly contain sponge and foam-based

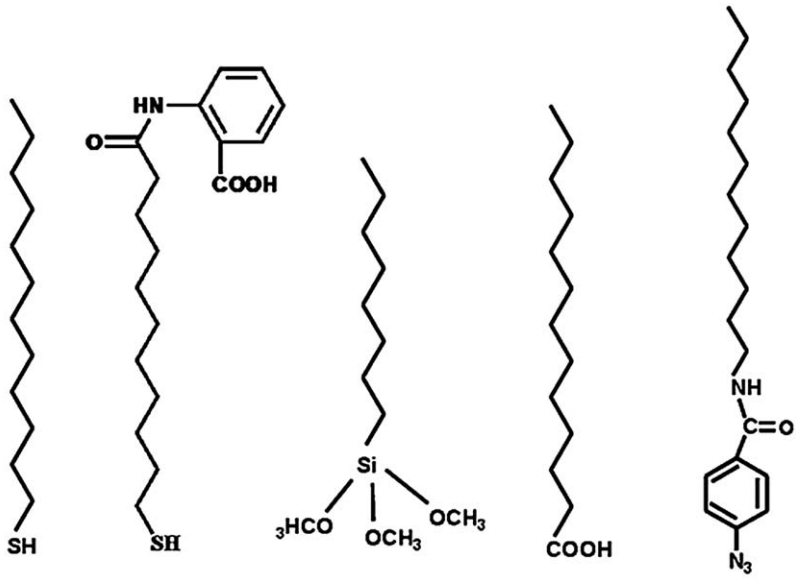

Figure 9.4 Examples of low-surface-energy modifications: long alkyl chain thiols, long alkyl chain thiols bearing benzoic acid, alkyl or fluorinated organic silanes, long alkyl chain fatty acids, and alkyl chain modified aromatic azides (from left to right).
Reproduced from ref. 29 with permission from the Royal Society of Chemistry.

materials, fabric-based materials, metallic mesh-based materials, particles and powdered materials.

9.2.3.1 Sponge and Foam-based Materials

Sponges and foams, with their inherently plentiful holes and hydrophilic properties, are cheaply available materials. Sponges and foams show an interconnected three-dimensional skeleton supported by chaotic fiber assemblies, thus endowing the sponges and foams with a huge space for oil absorption and storage. Generally, they can absorb various liquids (including water and oils or organics) with poor selectivity, which make them unrealistic for removing oils/organics from the water phase. Importantly, high selective absorption can be realized on a sponge after a construction of a befitting surface topography and modification with low surface energy substances. Pan *et al.* used a solution-immersion process to prepare superhydrophobic polyurethane (PU) sponges bearing a Ag coating.[36] They claimed that the as-prepared sponges quickly and selectively absorbed various kinds of oils over 13 times the sponges' weight while completely repelling water through a combination of porous, superhydrophobic, and superoleophilic properties. We have used a facile and easily scalable fabrication technique based on commercially available PU foams functionalized

with polypyrrole (PPy) by *in situ* polymerization. This sort of PPy-coated sponge comprising nano-scale rough coatings and micro-structured porous substrates is shown in Figure 9.5(a).[37] Such a superhydrophobic PPy-coated sponge is quite stable in several harsh conditions, including heating at 200 °C for 1 h, and freezing at −20 °C for 1 h. As shown in Figure 9.5(b), when the sponge was dropped on a *n*-hexane/water surface, it floated easily on the water and set out to absorb the red *n*-hexane quickly. By simply moving them around oil-polluted waters using tweezers, they can absorb the floating oil from the polluted regions, thereby purifying the contaminated water. In Figure 9.5(c), the underwater dichloroethane (higher density than water) can also be removed and recycled efficaciously using this superhydrophobic sponge. Endowed with a superhydrophobic property, sponge and foam-based materials are one of the promising routes for developing oil/water separation materials.

9.2.3.2 *Fabric-based Materials*

After endowing fabric with a superhydrophobic property, it is also considered a good candidate for oil/water separation because the ready-made fibers in the integral fabric provide microscale roughness and their native porosity ensures the free passage of liquids. It should be noted that the initial roughness of the fabric is not sufficient and establishing a hierarchical rough structured surface on the fabric is needed. Many research groups have utilized a dip coating method, one of the simplest approaches, to achieve this goal. Xue *et al.* have reported that by coating fibers with titania sol to generate a dual-size surface roughness, followed by hydrophobization with stearic acid, 1*H*,1*H*,2*H*,2*H*-perfluorodecyltrichlorosilane or their combination, hydrophilic cotton fabrics were made superhydrophobic.[38] We have proposed a general methodology for robust superhydrophobic fabrics *via* the *in situ* growth of both transition-metal oxides and metallic nanocrystals, including the simple neutralization reaction and oxidation–reduction reaction. The porous surfaces coated with Group VIII and IB nanocrystals (such as Fe, Co, Ni, Cu, and Ag) can not only present multiscale surface roughness, but also readily coordinate with thiols, leading to special wettability.[39] Frankly, fabric has its weakness, such as a thin, paper-like two-dimensional structure, which seriously limits its oil capture ability.

9.2.3.3 *Metallic Mesh-based Materials*

As important and irreplaceable engineering materials, metals are widely used in our daily life.[40] Metallic mesh-based materials possess relative uniform and different sizes of pores with different meshes (200, 400 or 800 meshes and so on) per square inch. There are many types of metallic mesh-based materials, such as stainless steel mesh, copper mesh, titanium mesh, *etc*. To enhance the superhydrophobic behavior of a porous metallic

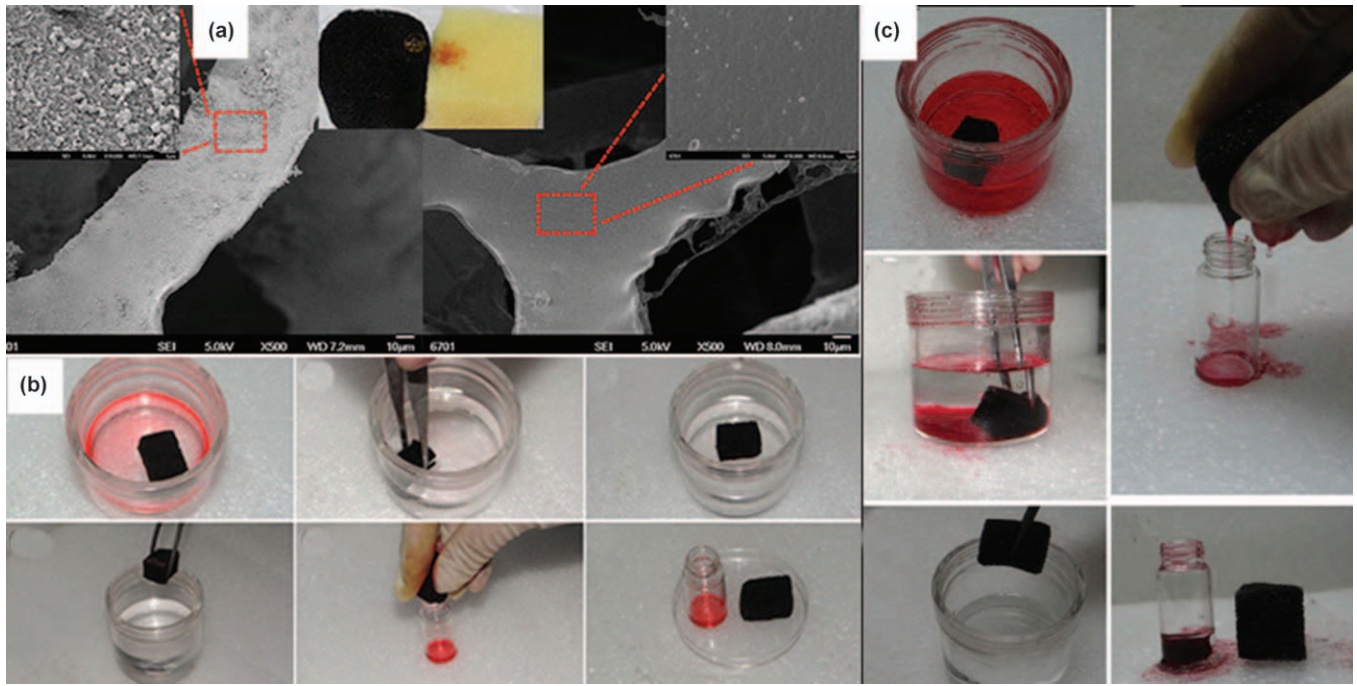

Figure 9.5 (a) SEM images of the superhydrophobic PPy-coated and pristine PU sponge. (b) The absorption and recycling process of *n*-hexane. (c) The absorption and recycling process of the underwater dichloroethane.
Reproduced from ref. 37 with permission from the Royal Society of Chemistry.

mesh film, a filtering mesh with selective permeability to water and oil was prepared, resulting in oil/water separating properties. A stainless steel mesh was the first material for fabricating superhydrophobic surfaces *via* a spray-and-dry method by Jiang *et al.* in 2004.[41] The pre-mixed aqueous emulsion containing Teflon, adhesive (polyvinyl acetate), dispersant (polyvinyl alcohol), and surfactant (sodium dodecyl benzene sulfonate) was sprayed evenly on the stainless mesh with compressed air and then it underwent a high-temperature drying process (350 °C) to decompose the adhesive, dispersant and surfactant. The prepared mesh was so water-repellent that a water droplet was unstable on it and rolled off easily We have reported that mixed modifiers of methyl-terminated thiol and carboxyl-terminated thiol were successfully assembled on stainless steel meshes utilizing polydopamine as the adhesion layer and the strong thiol ligand with Ag.[42] Importantly, the surfaces modified by mixed thiol show different responsive behavior to non-basic and basic water droplets. Plus, the selectiveness of high water–oil repellence reveals the unique and smart tendencies of the as-prepared functional stainless steel mesh.

Copper mesh is another frequently used substrate for oil/water separation. Inspired by a ramee leaf, rod-like unitary structured films were fabricated on copper meshes *via* a facile and simple chemical vapor corrosion method by us.[43] Following the surface modification of 1-decanethiol ($C_{10}H_{22}S$), the as-prepared films exhibiting superhydrophobicity and superoleophilicity can be applied to separate an oil–water mixture. In a comparative perspective, these superhydrophobic surfaces with unitary microstructures have better surface mechanical properties than those with binary micro- and nano-structures. Furthermore, we have fabricated a superhydrophobic copper mesh film, which can orderly separate the oil/water mixtures.[44] During the separation process, oil selectively permeated from water first, but then the water also spontaneously passed through later. For all we know, there has been no report about separating oil/water mixtures sequentially before. Compared to previous reports, it effectively simplifies the operation with no need for excluding water after oil separation. Besides, instead of making efforts to design materials responding to external stimuli (such as pH, temperature, UV, and magnetic field), it is much more simple to control the oil and water collection step by step *via* regulation of the oil/water mixture. What is more, the raw material used here is cheap, commercially available, and easily fabricated, which is of great importance to design an ideal separation material for industrial applications.

9.2.3.4 Particles and Powdered Materials

In the preceding subsections, the superhydrophobic surfaces used in water–oil separation were mainly fabricated on porous substrates, such as meshes, fabrics, membranes, and so on. These oil/water separation surfaces allow oil to penetrate through them whereas they resist water due to negative capillary effects. Although they can efficiently separate a mixture of oil and water, they

cannot selectively remove oil *in situ* from the oil–water interface. Recently, some novel hydrophobic and oleophilic particles without porous skeletons like sponges have been developed to achieve selective oil separation *in situ* from an oil/water mixture. Mahapatra *et al.* developed a simple, cost-effective and ''green'' route for the synthesis of highly hydrophobic and oleophilic $CaCO_3$ particles in the absence of any solvent and at ambient temperature conditions.[45] Oleic acid as an additive promotes polymorph selectivity from calcite to vaterite with ''flaky-floret'' like morphology with concomitant changes in its surface wettability from hydrophilic to hydrophobic. The materials synthesized have been successfully employed for selectively mopping up a variety of oils such as sunflower oil, engine oil and diesel from the surface of water. This has been established in its powder form as well as in the format of a ''spill-pouch''. In addition, the material has been used to fabricate functionalized polyurethane foam, which mops up oil spillages from water and renders the oil easy to recover. Although these particles and powders can be used in oil spill clean-ups, they are difficult to transfer and recycle. Naturally, magnetic particles/powders were developed to overcome the recycling problem because particles/powders with magnetism can be easily collected using an external magnetic field. We have reported a facile method to synthesize Fe_3O_4@polydopamine (Fe_3O_4@PDA) composite microspheres as shown in Figure 9.6.[1] These functional Fe_3O_4@PDA core–shell composite microspheres with magnetic response and special wetting properties were successfully assembled utilizing the modification of 1*H*,1*H*,2*H*,2*H*-perfluorodecyltrichlorosilane. In this paper, we demonstrated

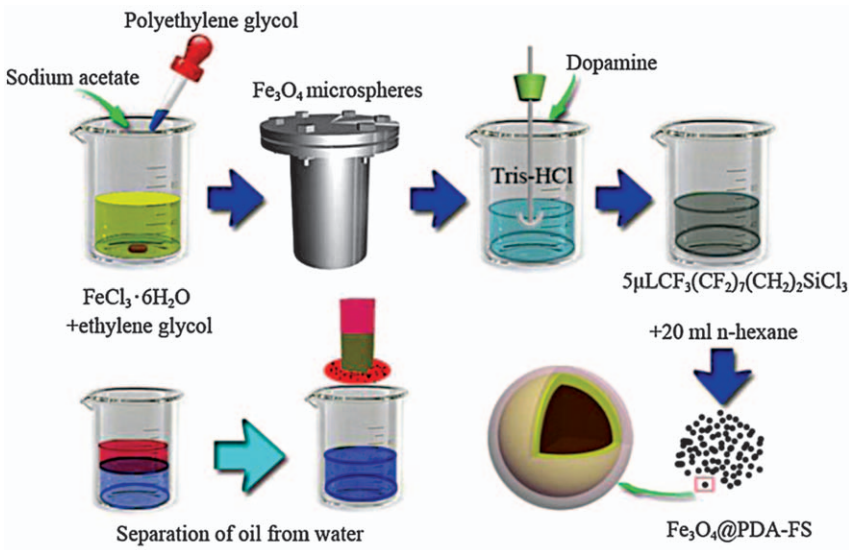

Figure 9.6 Schematic representation of the preparation and application of superhydrophobic Fe_3O_4@PDA-FS microspheres.

that the as-obtained product with designed functionality has favorable superhydrophobic and superparamagnetic properties, showing significant advantages in both magnetic control behavior and oil/water separation.

9.3 Various Oil–Water Separations Call for Various Superwettable Materials

Even superhydrophobic materials have been widely applied for oil–water separations, they cannot cover all this research field. As mentioned previously, we will expand to other extreme states of surface wettability, superhydrophilic/underwater superoleophobic surfaces. We should point out that the surfaces with superhydrophilic property often exhibit underwater superoleophobicity naturally and the difference between superhydrophobicity and superhydrophilicity is only whether the rough substrate is modified by low-surface-energy coatings or not. Here, we regard the superwettable materials with extreme states of surface wettability including superhydrophobic/superoleophilic materials and superhydrophilic/underwater superoleophobic materials.

9.3.1 The Background of Oil–Water Mixture Formation

Mixtures of oil and water can be classified in terms of the diameter (d) of the dispersed phase: free oil (oil droplet size >150 μm), dispersed oil (20 μm $<$ oil droplet size <150 μm), and emulsified oil (oil droplet size <20 μm).[46] Here, we denote the mixtures of oil and water with oil droplet size >150 μm as layered oil-and-water mixtures (or immiscible oil–water mixtures), and denote the mixtures of oil and water with oil droplet size <20 μm as emulsions. Utilizing the special wetting behavior of functional surfaces, two different types of these materials—superhydrophobic/superoleophilic surfaces and superhydrophilic/underwater superoleophobic surfaces—have been successfully designed, fabricated, and employed in the separation of layered oil–water mixtures, as given in Section 9.3.2.

Emulsions tend to have a cloudy appearance because the multiple phase-interfaces scatter light as they pass through the emulsion. An oil–water emulsion is a complex form of oil–water coexistence, especially in the presence of surfactants (or dispersants). Common emulsions are inherently unstable and, thus, do not tend to form spontaneously. Even to form a temporary emulsion, energy input through stirring, homogenizing, shaking, or exposure to power ultrasound is needed. Over time, emulsions tend to revert to the stable states of the phases comprising tiny parts of emulsion. To obtain a stable state of emulsions, an emulsifier (or surfactant), a substance with both hydrophobic and hydrophilic groups, which stabilizes an emulsion by increasing its kinetic stability, are necessary.

Despite this, oily wastewater, whether industrial effluent or sanitary wastewater, exists in emulsion form. So the separation of oil–water emulsions has a double significance in ecology and economics, and special

attention is paid to the latest development in advanced materials for oil–water emulsion separation below.

9.3.2 Types of Superwettable Surfaces Applied for Immiscible Oil–Water Separations

9.3.2.1 Superhydrophobic/Superoleophilic Surfaces Applied for Oil–Water Separations

Due to the lower surface tension of oil, it is usually hard for the superhydrophobic surfaces to repel oil droplets and in many cases, superhydrophobic surfaces exhibit a superoleophilic property. Superhydrophobic–superoleophilic materials are typical oil-removing materials. The superhydrophobic and superoleophilic properties will make an oil phase spread easily while the water phase will be repelled, thus separating oils from an oil–water mixture. These types of ideal oil removing materials are generally considered to have a high oil absorption capacity as well as a low water pick up, low density, they are environmentally friendly, and have good recyclability for a wide range of oils/organics.

We have presented that stable superhydrophobic and superoleophilic nanocoatings on textiles and sponges, successfully achieved from thiol-ligand nanocrystals, can effectively be used for application in oil/water separation.[47] The nanocrystals include VIII and IB metals and oxide nanoparticles, such as Fe, Co, Ni, Cu and Ag. Textiles with superhydrophobic VIII and IB nanocoatings with *n*-octadecyl thiol as a modifier have a similar surface energy to oil droplets, and these modified textiles will favor superoleophilicity. The difference between water and oil on these surfaces with special wettability results in one intrinsic application in oil/water separation.

We have developed a kind of stable superhydrophobic/superoleophilic soft porous material for oil/water separation *via* the oxidative chemical polymerization of aniline on the surface of fabrics as shown in Figure 9.7(a).[48] Interestingly, the as-prepared fabrics showed stable and robust superhydrophobic properties towards many corrosive solutions (acidic, basic, salt liquids), hot water, and mechanical abrasion. In addition, it was proven that this method can also be applied to other porous materials with different pore diameters and chemical composition, such as stainless steel meshes with different pore diameters and sponges. As shown in Figure 9.7(b), when a mixture of water and oil (dyed with Solvent Red 24 for clear observation) was poured from a separating funnel onto a mesh, the water flowed to the outside of the bottle into the beaker, while oil quickly permeated though the mesh and dropped into the bottle. The results indicated that the oil/water mixture could be effectively separated by the as-prepared superhydrophobic PANI-coated mesh. Importantly, oil/water separation has successfully been achieved *via* the superhydrophobic/superoleophilic PANI-coated fabric, as illustrated in Figure 9.7(c). When the hexane and water mixture was poured onto the superhydrophobic fabric,

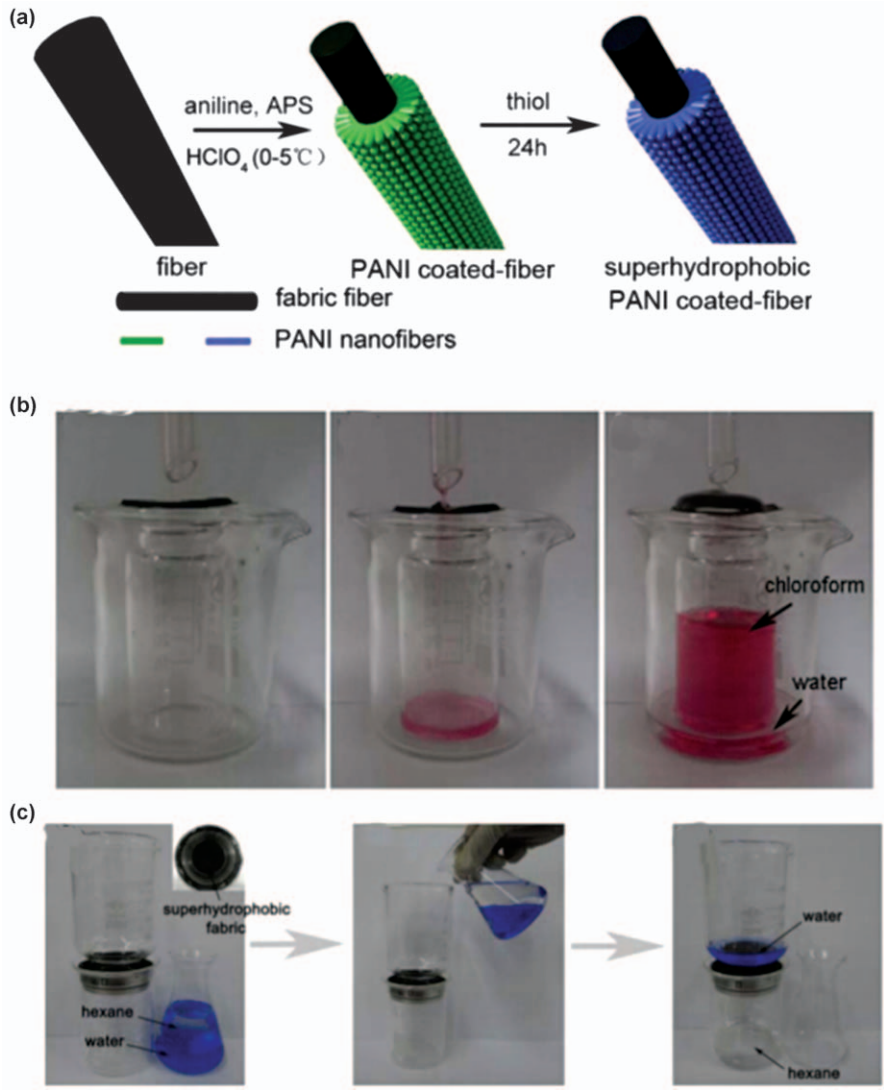

Figure 9.7 (a) Schematic drawing of the synthesis procedure of the superhydrophobic PANI-coated fabric. (b) Oil/water separation process of the superhydrophobic mesh coated with PANI nanofibers; the chloroform was dyed with Solvent Red 24 for clear observation. (c) Oil/water separation process of hexane and water using the superhydrophobic PANI-based fabric; the water was dyed by methylene blue for clear observation. Reproduced from ref. 48 with permission from the Royal Society of Chemistry.

hexane quickly spread and permeated through the fabric and then rapidly dropped into the beaker underneath, whereas the water (dyed by methylene blue for clear observation) resided on the fabric.

9.3.2.2 *Superhydrophilic/Underwater Superoleophobic Surfaces Applied for Oil–Water Separations*

Gradually, researchers have discovered some drawbacks of superhydrophobic/superoleophilic materials, *i.e.*, they are easily fouled or blocked by oil due to high viscosity and these materials are usually unsuitable for oils that are less dense than water. Fish scales, which are known to be well protected from contamination by oil pollution in the sea, have stimulated particular interest. Inspired by fish scales, a promising oil–water separation material with hydrophilic and underwater superoleophobic properties has been developed. Superhydrophobic/superoleophilic materials are applied to allow the oil phase to penetrate the surface (or absorb the oil phase) but repelling water while superhydrophilic and underwater superoleophobic surfaces can let the water pass through freely, however repelling oil totally. In 2014, our group achieved some good results regarding this aspect. Dong *et al.* demonstrated a novel method to fabricate a hydrophilic graphene oxide (GO) coating onto stainless steel meshes.[49] Compared to neat meshes, GO-coated meshes become more hydrophilic in air and superoleophobic under water. Taking advantage of this completely opposite wettability, it can separate various oils from water under gravity. Yu *et al.* reported an outstanding superhydrophilic and underwater superoleophobic film that can separate water from oil prepared by growing pure silica zeolite crystals on a stainless steel mesh.[50] Based on the excellent superhydrophilicity and underwater superoleophobicity of their zeolite surface, high separation efficiency of various oils can be achieved. Flux and intrusion pressure are tunable by simply changing the pore size, dependent on the crystallization time of the zeolite crystals. Based on an important type of zeolite (Silicalite-1: structure type MFI) coating on the stainless steel, we have prepared special wettable films that are superamphiphilic in air and superoleophobic underwater as shown in Figure 9.8.[51] This prepared film can effectively collect the oil from an oil/water mixture underwater driven by gravity several times, showing good durability and high separation efficiency, which is very helpful in the promising application of energy-efficient membranes for reducing the environmental impact of oil spills.

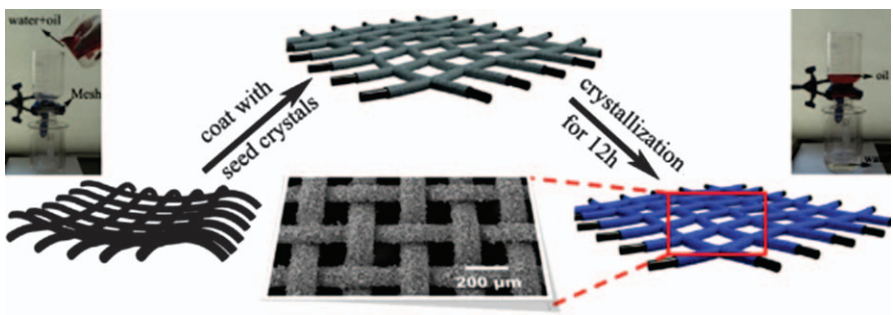

Figure 9.8 Superhydrophilic and underwater superoleophobic MFI zeolite-coated film for oil/water separation.

9.3.3 Superwettable Surface Applied for Emulsified Oil–Water Separations

In realistic situations, oil–water mixtures are not always well layered and a large amount of oil–water mixtures needed to be processed exists in the form of an emulsion. The materials mentioned above are commonly not suitable for emulsified oil/water separation, especially for surfactant-stabilized emulsions. The pore sizes of these materials are usually tens of micrometers. However, the oil dispersion phase in water or water dispersion phase in oil are generally considered as automatic layers because oil and water are immiscible in nature and their densities are different. Generally, an emulsion is defined as a drop in the diameter of the dispersed phase (oil or water) lower than 20 μm. Here, we defined an oil dispersion phase in a water continuous phase (size of oil droplet less than 20 μm) as an ''oil-in-water emulsion'' and defined a water dispersion phase (size of water droplet less than 20 μm) in an oil continuous phase as ''water-in-oil emulsion''. Whether an emulsion of oil and water turns into an ''oil-in-water emulsion'' or a ''water-in-oil emulsion'' depends on the volume fraction of both and the type of emulsifier (surfactant) present. Some progress has been made in this field and the emulsion separation materials can also be divided into the same types as the layered oil/water separation materials: superhydrophobic/superoleophilic materials and superhydrophilic/underwater superoleophobic materials.

9.3.3.1 Superwettable Surface Applied for Emulsified Oil-in-water Separations

Chen *et al.* report a novel kind of superhydrophilic hybrid membrane, prepared by depositing a $CaCO_3$-based mineral coating on PAA-grafted polypropylene microfiltration membranes, for effective oil-in-water emulsion separation.[52] In their work, diesel was utilized as the target oil for preparing oil-in-water emulsions. Experimental results show that the permeate flux can reach 2000 L m^{-2} h^{-1}. This value is much higher than conventional ultrafiltration membranes (300 L m^{-2} h^{-1}), while the external pressure used (0.05 MPa) is lower than that of the latter (>0.1 MPa).

In Wang's work, they synthesized a hierarchically porous monolith with macro- and meso-pores *via* a sol–gel and phase separation process.[53] Due to the surface modification by organic silanes, the wettability of the silica material was effectively controlled. A series of hydrophobic porous silica monoliths (HPSM) were obtained. Using a ''reverse membrane emulsification'' process, the HPSM not only cleared oil away from water, but also broke the micro-emulsion efficiently, even when emulsion stabilizer was in the system, as shown in Figure 9.9. They speculated that HPSM exhibited excellent demulsification ability *via* adsorbing the emulsifier from the emulsion, leading to the complete breakdown of surfactant stabilized emulsions (Figure 9.9(c)). The demulsification ratio is as high as 99.95% and the HPSM were reusable.

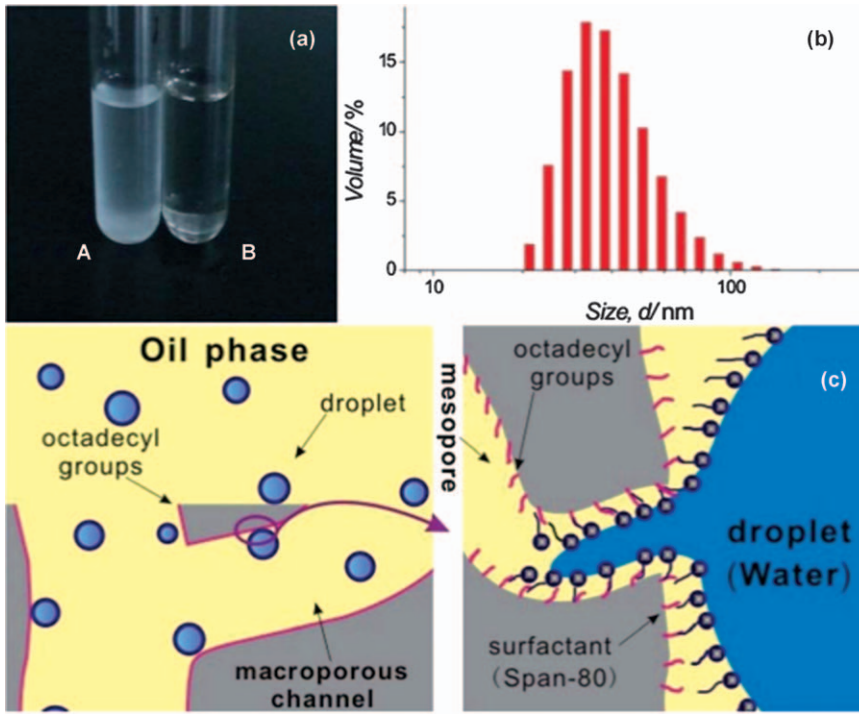

Figure 9.9 (a) Image of the filtrated solutions which were partly, A, and completely, B, demulsified. (b) The diameter distribution of droplets in the micro-emulsion and (c) the mechanism of the demulsification by HPSM-18. Reproduced from ref. 53 with permission from the Royal Society of Chemistry.

9.3.3.2 *Superwettable Surface Applied for Emulsified Water-in-oil Separations*

Amar *et al.* have prepared one kind of fluorosilane-grafted ceramic membranes that can be used to separate waterin-oil emulsions, through a thermally-driven separation process.[54] After grafting 1*H*,1*H*,2*H*,2*H*-perfluorodecyltriethoxysilane on the ceramic membrane, their hydrophilic character (CA = 25°) changed into hydrophobic (CA = 160°). High salt and oil retention higher than 99% were obtained using a modified ceramic membrane. Huang *et al.* developed a novel fluorinated benzoxazine, namely 3-(3-(trifluoromethyl)phenyl)-2*H*-benzoxazine-6-carbaldehyde (BAF-CHO) as a starting monomer, which was synthesized *via* a one-step Mannich reaction.[55] The as-synthesized *in situ* polymerized superhydrophobic and superoleophilic nanofibrous membranes can effectively separate water-in-oil microemulsions, as schematically shown in Figure 9.10, which exhibit an extremely high flux of 892 L m^{-2} h^{-1} solely driven by gravity, as well as good antifouling properties, thermal stability and durability, suggesting their use as promising materials

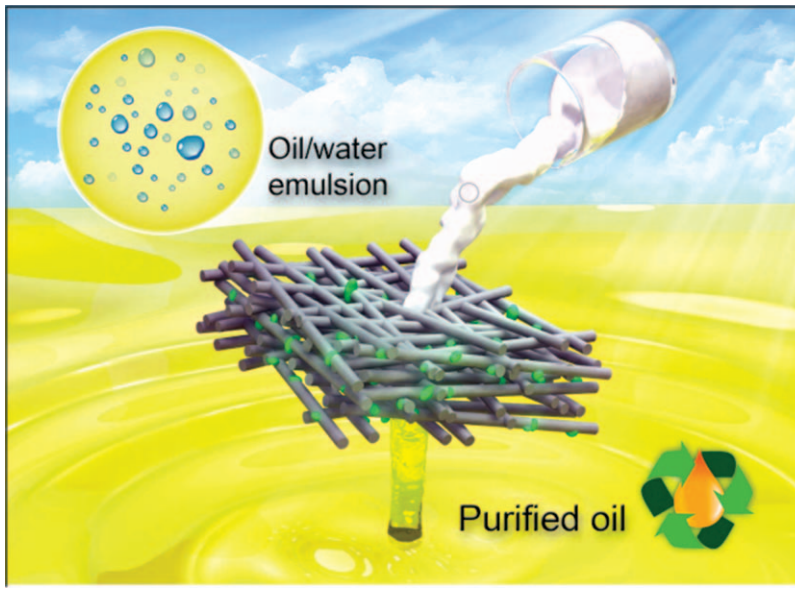

Figure 9.10 Schematic of the emulsified water–oil separations from Huang's work. Reproduced from ref. 55 with permission from the Royal Society of Chemistry.

for practical emulsified wastewater treatment. (Even though the phrase ''oil/water emulsion'' is used in the picture, the microemulsion is an water-in-oil emulsion as the partially enlarged drawing in the image indicates.)

Zhang and Chen *et al.* prepared superhydrophobic polymer/carbon nanotube hybrid membranes *via* covalent attachment of a hydrophobic polymer.[56] The membrane obtained shows excellent separation properties for surfactant-stabilized water-in-oil emulsions with separation efficiency as high as 99.94% and high flux (5000 L m^{-2} h^{-1} bar^{-1}). As shown in Figure 9.11, a dispersed water/toluene emulsion was poured into the filtration cell and was suction filtered under a pressure of 10 kPa. Emulsion droplets de-emulsified once touching the PS-g-CNTs membrane, toluene immediately permeated through the membrane and water was retained above the membrane. In Figure 9.11(b), before separating, there are numerous water droplets with a size of about 70 nm in the feed solution. In Figure 9.11(c), after separating, there are no droplets that can be observed in the collected filtrate in the whole view. All this evidence demonstrates the excellent separating properties of the PS-g-CNTs membrane. It is worth noting that the membrane exhibited good antifouling properties, outstanding recyclability, robust stability and durability, showing attractive potential for practical oil/water separation.

In realistic situations, oily water produced and emitted by human activities or industries are extremely complex situations regarding the coexistence of oil-in-water emulsions and water-in-oil emulsions. It is hard to judge

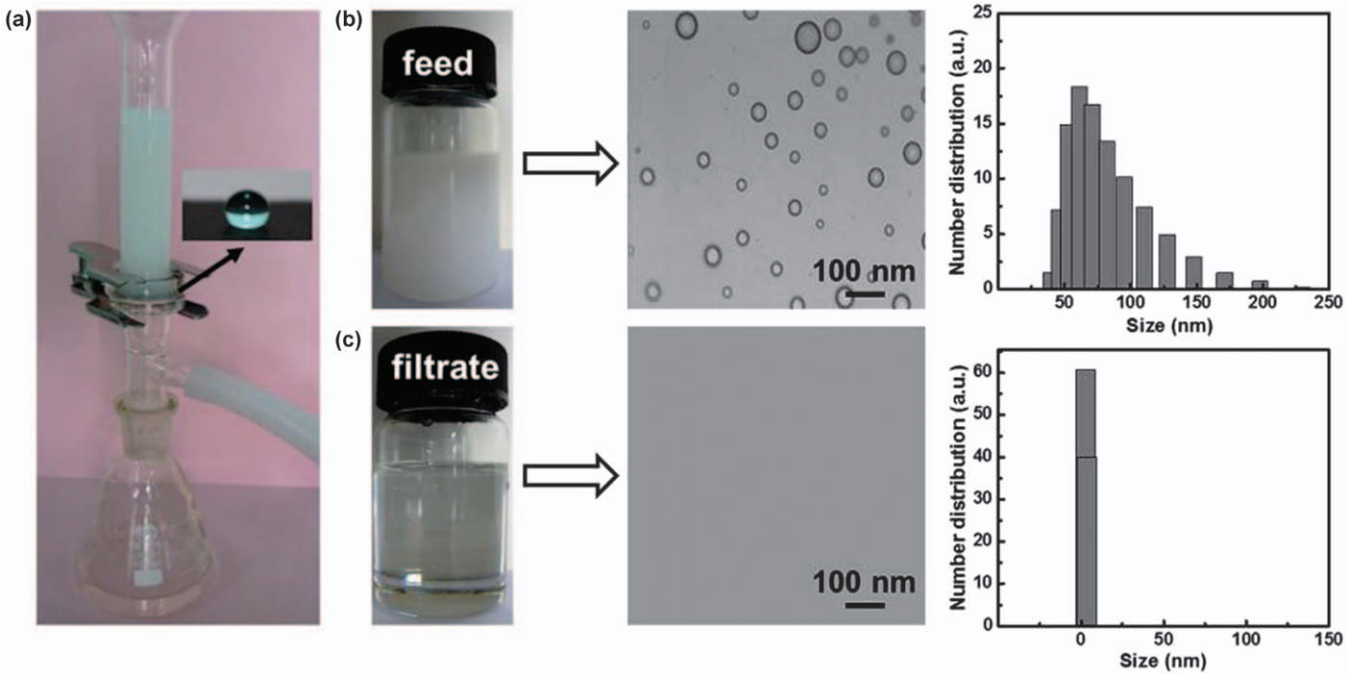

Figure 9.11 (a) Photograph of separating a water/toluene emulsion where toluene selectively permeates through the PS-CNTs membrane. Photographs and DLS data of water/toluene emulsion before (b) and after (c) filtration. Reproduced from ref. 56 with permission from the Royal Society of Chemistry.

their kind and, in most cases, there is probably a mixture of these two types. Killing two birds with one stone is interesting and satisfying. Therefore, it is of great importance to seek better functional materials in response to these circumstances. Gu *et al.* achieved Janus (with different properties on the same object) polymer/CNTs hybrid membranes *via* self-initiated photo-grafting and photopolymerization (SIPGP).[57] This novel membrane can effectively separate both surfactant stabilized oil-in-water and water-in-oil emulsions because of the anisotropic wettability of the membranes. The WCA of the membrane increases to 153° after modification with hydrophobic poly(styrene) (PS); on the other hand, grafting hydrophilic poly(*N*,*N*-dimethylaminoethyl methacrylate) (PDMAEMA) from the lower surface (opposite side of the PS brushes) leads to a WCA decreasing to 17°. These remarkable membranes make them promising candidates for various practical applications such as controllable oil/water separation and selective oil absorption.

9.4 The Principles to Optimal Design of Oil–Water Separations Materials

In essence, oil/water separation is the wettability behavior that occurs at the interface of the solid, air, water and oil phase. When a liquid droplet was presented on a solid surface in air, we investigated a series of situations. Theoretically, we have optimally designed superhydrophobic surfaces using a paraboloid and semicircular protrusion microtexture.[58] The effects of all the geometrical parameters for such a paraboloid microtexture on free energy (FE) and free energy barrier (FEB) as well as equilibrium contact angle (ECA) and contact angle hysteresis (CAH) of a superhydrophobic surface have been systematically investigated in detail. We found that the droplet position for a metastable state is closely related to the intrinsic CA of the surface. Furthermore, the paraboloid base steepness plays a significant important role in ECA and CAH, and a critical steepness is necessary for the transition from non-composite to composite states. In addition, it has been revealed experimentally that some superhydrophobic surfaces in nature, such as the rice leaf, show strong anisotropic wetting behavior. In our published work, based on a thermodynamic approach, the effects of the profile shape of a parallel grooved microstructure on FE with its barrier (FEB) and ECA with its hysteresis (CAH) for various orientations of different parallel micro texture surfaces have been systematically investigated in detail.[59] The results indicated that the anisotropy of wetting properties strongly depended on the specific topographical features and wetting state.

To easily understand wetting behavior underwater, we firstly and comparatively give the multi-situations in air (Figure 9.12(a)–(c)). When wetting behavior occurs underwater, we take the CA of a smooth surface into account firstly (Figure 9.12(d)). As suggested by Jung and Bhushan, the wetting equation at a solid–water–oil interface can be conducted by combining the Young's equation (eqn (9.1)) of a solid–air–water interface and a

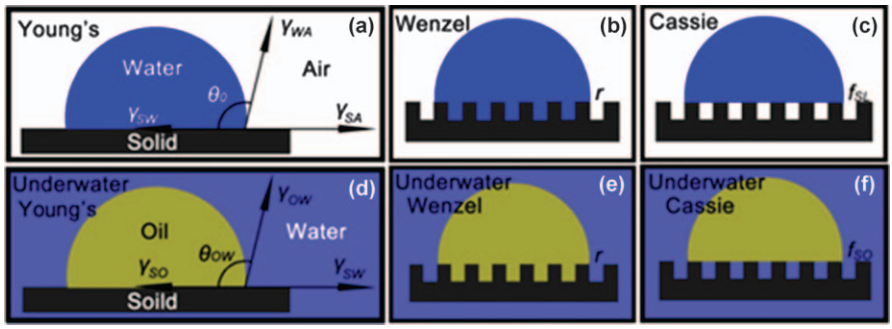

Figure 9.12 Comparative illustration of the in-air and underwater wetting mechanism of water/oil droplets residing on solid surfaces at different wetting states. (a) Water droplet on a smooth surface. Water droplet on rough surfaces with (b) a Wenzel (homogeneous) wetting state and (c) a Cassie (heterogeneous) wetting state. (d) Underwater oil droplets on a smooth surface. Underwater oil droplets on rough surfaces with (e) a Wenzel (homogeneous) wetting state and (f) a Cassie (heterogeneous) wetting state.
Reproduced from ref. 61 with permission from the Royal Society of Chemistry.

solid–air–oil interface.[60] The apparent OCA (θ_{OW}) in an aqueous environment can be given as:

$$\cos\theta_{OW} = \frac{\gamma_{OA}\cos\theta_O - \gamma_{WA}\cos\theta_W}{\gamma_{OW}} \tag{9.5}$$

where θ_W and θ_O are the WCA and OCA in air. γ_{OA}, γ_{WA} and γ_{OW} are interface tensions of oil–air, water–air and oil–water interfaces, respectively. θ_W and θ_O represent the WCA and OCA in air. As predicted by eqn (9.5), for a hydrophilic surface, the surface is simultaneously oleophilic due to the lower surface tension of oil (γ_{OA}) in air than that of water (γ_{WA}) ($\theta_O < \theta_W < 90^\circ$). Therefore, the values of $\cos\theta_O$ and $\cos\theta_W$ are all positive. Since the surface tensions of oil/organic liquids are much lower than that of water ($\gamma_{OA} \ll \gamma_{WA}$), the value of $\gamma_{OA}\cdot\cos\theta_O - \gamma_{WA}\cdot\cos\theta_W$ is commonly negative and thus it can be concluded that most hydrophilic surfaces in air show an oleophobic property underwater at the solid–water–oil interface.

Similar to the Wenzel and Cassie equations in air, the underwater Wenzel equation (Figure 9.12(e)) and Cassie equation (Figure 9.12(f)) can be obtained by introducing the surface roughness and contact phase fractions (solid–oil and solid–water interfaces).

$$\text{Wenzel equation: } \cos\theta_W = r\cos\theta_{OW} \tag{9.6}$$

$$\begin{aligned}\text{Cassie equation: } \cos\theta_{CB} &= r_f f_{SO}\cos\theta_{OW} + f_{SO} - 1 \\ &= r_f\cos\theta_{OW} - f_{SW}(r_f\cos\theta_{OW} + 1)\end{aligned} \tag{9.7}$$

where f_{SO} is the solid–oil fraction under the contact area. It is obvious that the underwater wettability of oil is also determined by the surface roughness, solid–oil fraction (solid–water fraction), as well as the Young's CA of oil in an aqueous environment.

The above analysis is of great concern to optimally separate layered oil/water mixtures. As for oil/water emulsion separation, more factors should be taken into account and a size-sieving mechanism is the foundation model. Except that the wettability of the membrane must be controlled in a certain range, the pore sizes of the filtering membrane are the key factors. To make the continuous phase pass through the membrane quickly, the pore sizes must be large enough. To avoid droplets of the dispersed phase squeezing through the pores, the size of the pores must be small enough as shown in Figure 9.13.

To quantitatively estimate the speed of continuous phase passing through the membrane, a classical fluid dynamic theory is the Hagen–Poiseuille equation:[63]

$$J = \frac{\varepsilon \pi r_p^2 \Delta p}{8 \mu L} \tag{9.8}$$

where the filtration rate J is described as a function of the surface porosity ε, the membrane's pore radius r_p, the pressure drop Δp, the viscosity of the liquid μ, and the total distance L of the liquid running through the membrane.[62] This equation predicts that the flux is directly proportional to the square of the pore size of the membrane and inversely proportional to the thickness of the membrane. So, we should work on trying to prepare thinner membranes with an optimal pore size.

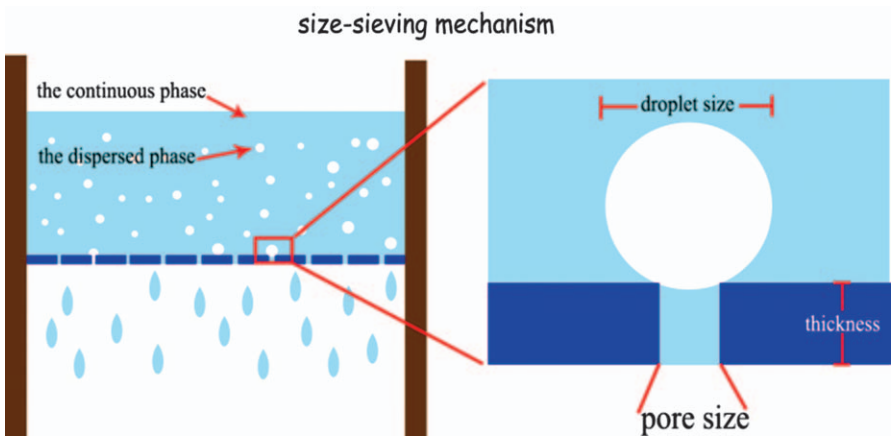

Figure 9.13 A schematic diagram of the size-sieving mechanism. Reproduced from ref. 62 with permission from the Royal Society of Chemistry.

However, if the filtering membrane is too thin, then the problem of mechanical strength would stand out. Here, we introduce two important performance assessments for the filter membrane: trans-membrane pressure (P_T) and breakthrough pressure (P_B). P_T is the external pressure on the separation system and the flux increases linearly with increasing the P_T. However, the maximum P_T that a certain membrane can bear is limited by its mechanical strength. The P_B is the maximum pressure at which the filtering membranes still possess permselectivity. Also, the external P_T has the risk of exceeding the oil P_B. In this case, both the continuous phase and emulsions are forced to permeate through the membranes, decreasing the separation efficiency. Theoretically, the relationship between these parameters can be expressed as follows:[64]

$$P_B = \frac{2\gamma_{wo}\cos\theta_{adv,ws(o)}}{r_p} \tag{9.9}$$

$$Q = \frac{-kA}{4\mu}\frac{\Delta P}{L} \sim r^4 \tag{9.10}$$

$$Q_{max} = \frac{\rho_p A \gamma_{wo}\pi\cos\theta_{adv,ws(o)}}{4\mu}\frac{r_p^3}{L} \tag{9.11}$$

Here Q_{max} is the maximum flow rate while still rejecting emulsions, ρ_p is the number pore density, A is the area of the membrane, γ_{wo} is the interfacial tension between water and oil, and $\cos\theta_{adv,ws(o)}$ is the advancing contact angle of a water droplet on the membrane surface in the presence of oil. These equations explicitly reveal how flow rate is increasingly limited for decreasing pore sizes and how the surface wettability, membrane diameter, permeability and pressure will affect the maximum flow. For the optimal design of superwettable materials applied to oil/water mixtures, we can benefit a lot from these principles.

9.5 Summary and Outlook

Nowadays, oil–water separation is a worldwide issue and challenge due to the increasing amount of industrial oily wastewater and polluted oceanic waters, as well as frequent oil spill accidents. Oil-contaminated water needs to be addressed urgently. Traditional techniques such as oil skimmers, centrifuges, depth filters, coalescers, and flotation technologies often take a long time and need tedious manual operation. These separation processes of an oil/water mixture are empirical to a great extent, thus making the separation incomplete with either oil remaining in water or water remaining in oil. So more feasible methods should be improved to separate oil/water mixtures. Also, a higher flow rate, better selectivity, and excellent separation efficiency are required to meet the rapid demands.

Superhydrophobic or other special wettability materials show enormous potential in the treatment of oil spill accidents and industrial oily water due to their high selective absorbing/filtering features. We begin with the understanding and design of superhydrophobic surfaces. In this chapter, we have introduced their origin and definition, approaches to superhydrophobic surfaces and endowing porous materials or particles with superhydrophobic properties that have potential ability for separating oil/water mixtures. Next, we reviewed recent progress in superhydrophobic/superoleophilic surfaces and superhydrophilic/underwater superoleophobic surfaces applied for separating layered oil/water mixtures. These materials used for the separation of immiscible oil–water mixtures are usually not effective for emulsified oil–water mixtures, especially not for surfactant-stabilized micro emulsions with a dispersed droplet size below 20 μm. Recently reported membrane technologies based on superwettable materials with potential for efficient separation of emulsified oil–water mixtures were highlighted by sorting them into two categories: separation of oil-in-water or water-in-oil emulsions.

Although the investigations in this field have made tremendous strides, there are still a lot of challenges, and some of the problems still need to be solved, such as separation efficiency, flow rate and service life. In theory, we have pointed out the underlying mechanism to improve the performance of oil/water separation.

To achieve the industrialization of oil/water separation materials at an early stage, future work will mainly concentrate on aspects as follows from our viewpoint. First and foremost, the design and synthesis of stable and durable superhydrophobic materials are the key issues. To obtain an extreme wetting state, most of the superhydrophobic surfaces are elaborated with micro and nano-scale fine structures, which can be easily damaged by external influences including mechanical stress and chemical contamination, restricting the material's practical applications. Secondly, the simple and mass-production techniques of oil/water separation materials for large-area oil spills are still required. A large portion of the synthesis methods cannot be carried out on a large scale, such as the hydrothermal method, electrochemical deposition and the *in situ* growth method. Thirdly, it is challenging to realize effective and high-throughput separation of a wide range of oil/water emulsions with small droplet sizes from the micrometer to the nanometer range, because the separation speed and the membrane pore sizes are considered to be contradictory. Fourthly, separation of high-viscous oil/water mixtures is glamorous and should be taken into consideration. Last but not the least, smart interfacial materials for different oil/water separation purposes are also needed to be put forward. These smart interfacial materials are external stimulus-responsive, ranging from single to dual or multiple stimulus-responsive.

Acknowledgements

This work is supported by the National Nature Science Foundation of China (NO11172301 and 21203217), the ''Funds for Distinguished Young

Scientists'' of Hubei Province (2012FFA002), the ''Western Light Talent Culture'' Project, the Co-joint Project of Chinese Academy of Sciences and the ''Top Hundred Talents'' Program of Chinese Academy of Sciences and the National 973 Project (2013CB632300). Many thanks to Mr Ben Wang and Yifan Si for thoughtful discussions and kind help.

References

1. F. Yang, Y. Dong and Z. Guo, *Colloids Surf., A*, 2014, **463**, 101–109.
2. (a) J. F. Piatt and P. Anderson, *Response of Common Murres to the Exxon Valdez Oil Spill and Long-term Changes in the Gulf of Alaska Marine Ecosystem*, ed. S. D. Rice, R. B. Spies, D. A. Wolfe and B. A. Wright, 1996, vol. 18, pp. 720–737; (b) C. H. Peterson, S. D. Rice, J. W. Short, D. Esler, J. L. Bodkin, B. E. Ballachey and D. B. Irons, *Science*, 2003, **302**, 2082–2086.
3. P. Lin and L. Guo, *Mar. Chem.*, 2015, **174**, 13–25.
4. Z. Chu, Y. Feng and S. Seeger, *Angew. Chem., Int. Ed.*, 2015, **54**, 2328–2338.
5. G. Kwon, A. K. Kota, Y. Li, A. Sohani, J. M. Mabry and A. Tuteja, *Adv. Mater.*, 2012, **24**, 3666–3671.
6. Z. Xue, S. Wang, L. Lin, L. Chen, M. Liu, L. Feng and L. Jiang, *Adv. Mater.*, 2011, **23**, 4270–4273.
7. J. Rubio, M. L. Souza and R. W. Smith, *Miner. Eng.*, 2002, **15**, 139–155.
8. S. Wang, K. Liu, X. Yao and L. Jiang, *Chem. Rev.*, 2015, **115**, 8230–8293.
9. (a) B. Wang, Y. Zhang, L. Shi, J. Li and Z. Guo, *J. Mater. Chem.*, 2012, **22**, 20112; (b) F. Yang and Z. Guo, *J. Bionic Eng.*, 2015, **12**, 88–20197.
10. V. A. Ganesh, H. K. Raut, A. S. Nair and S. Ramakrishna, *J. Mater. Chem.*, 2011, **21**, 16304–16322.
11. Z. Chu and S. Seeger, *Chem. Soc. Rev.*, 2014, **43**, 2784–2798.
12. T. Darmanin and F. Guittard, *J. Mater. Chem. A*, 2014, **2**, 16319–16359.
13. Z. Guo and W. Liu, *Plant Sci.*, 2007, **172**, 1103–1112.
14. X. Gao and L. Jiang, *Nature*, 2004, **432**, 36.
15. S. Yu, Z. Guo and W. Liu, *Chem. Commun.*, 2014, **51**, 1775–1794.
16. C.-H. Xue and J.-Z. Ma, *J. Mater. Chem. A*, 2013, **1**, 4146–4161.
17. T. Jiang, Z. Guo and W. Liu, *J. Mater. Chem. A*, 2014, **3**, 1811–1827.
18. Z. Guo, F. Zhou, J. Hao and W. Liu, *J. Am. Chem. Soc.*, 2005, **127**, 15670–15671.
19. X. Zhu, Z. Zhang, X. Xu, X. Men, J. Yang, X. Zhou and Q. Xue, *J. Colloid Interface Sci.*, 2012, **367**, 443–449.
20. J. Yong, F. Chen, Q. Yang, D. Zhang, U. Farooq, G. Du and X. Hou, *J. Mater. Chem. A*, 2014, **2**, 8790–8795.
21. H.-B. Jo, J. Choi, K.-J. Byeon, H.-J. Choi and H. Lee, *Microelectron. Eng.*, 2014, **116**, 51–57.
22. S. Barthwal, Y. S. Kim and S.-H. Lim, *J. Colloid Interface Sci.*, 2013, **400**, 123–129.
23. B. Wang and Z. Guo, *Appl. Phys. Lett.*, 2013, **103**, 063704.

24. H. Wang and Z. Guo, *Appl. Phys. Lett.*, 2014, **104**, 183703.
25. Y. Si and Z. Guo, *Nanoscale*, 2015, **7**, 5922–5946.
26. Y. Li, G. Duan and W. Cai, *J. Colloid Interface Sci.*, 2007, **314**, 615–620.
27. B. Dong, D. Fan, S. Wang and Z. Guo, *Chem. Lett.*, 2015, **44**, 1245–1247.
28. H. Bellanger, T. Darmanin, E. Taffin de Givenchy and F. Guittard, *Chem. Rev.*, 2014, **114**, 2694–2716.
29. X. Zhang, F. Shi, J. Niu, Y. Jiang and Z. Wang, *J. Mater. Chem.*, 2008, **18**, 621–633.
30. B. Wang and Z. Guo, *Chem. Commun.*, 2013, **49**, 9416–9418.
31. Y. Si, H. Zhu, L. Chen, T. Jiang and Z. Guo, *Chem. Commun.*, 2015, **51**, 16794–16797.
32. J. Zhang, Y. Liu, Z. Wei and J. Zhang, *Appl. Surf. Sci.*, 2013, **265**, 363–368.
33. F. Shi, J. Niu, Z. Liu, Z. Wang, M. Smet, W. Dehaen, Y. Qiu and X. Zhang, *Langmuir*, 2007, **23**, 1253–1257.
34. X. Zhu, Z. Zhang, X. Xu, X. Men, J. Yang, X. Zhou and Q. Xue, *Langmuir*, 2011, **27**, 14508–14513.
35. B. Xin and J. Hao, *Chem. Soc. Rev.*, 2010, **39**, 769–782.
36. Q. Zhu, Q. Pan and F. Liu, *J. Phys. Chem. C*, 2011, **115**, 17464–17470.
37. S. Yu and Z. G. Guo, *RSC Adv.*, 2015, **5**, 107880–107888.
38. C.-H. Xue, S.-T. Jia, H.-Z. Chen and M. Wang, *Technol. Adv. Mater.*, 2008, **9**, 035001.
39. B. Wang, J. Li, G. Wang, W. Liang, Y. Zhang, L. Shi, Z. Guo and W. Liu, *ACS Appl. Mater. Interfaces*, 2013, **5**, 1827–1839.
40. J. Guo, S. Yu, J. Li and Z. Guo, *Chem. Commun.*, 2015, **51**, 6493–6495.
41. L. Feng, Z. Zhang, Z. Mai, Y. Ma, B. Liu, L. Jiang and D. Zhu, *Angew. Chem., Int. Ed.*, 2004, **43**, 2012–2014.
42. F. Yang and Z. Guo, *RSC Adv.*, 2015, **5**, 13635–13642.
43. H. Zhu and Z. Guo, *Chem. Lett.*, 2014, **43**, 1645–1647.
44. H. Zhu and Z. Guo, *Chem. Lett.*, 2015, **44**, 1431–1433.
45. A. Sarkar and S. Mahapatra, *J. Mater. Chem. A*, 2014, **2**, 3808–3818.
46. Y. Zhu, F. Zhang, D. Wang, X. F. Pei, W. Zhang and J. Jin, *J. Mater. Chem. A*, 2013, **1**, 5758–5765.
47. J. Li, L. Shi, Y. Chen, Y. Zhang, Z. Guo, B.-L. Su and W. Liu, *J. Mater. Chem.*, 2012, **22**, 9774.
48. W. Liang and Z. Guo, *RSC Adv.*, 2013, **3**, 16469–16474.
49. Y. Dong, J. Li, L. Shi, X. Wang, Z. Guo and W. Liu, *Chem. Commun.*, 2014, **50**, 5586–5589.
50. Q. Wen, J. Di, L. Jiang, J. Yu and R. Xu, *Chem. Sci.*, 2013, **4**, 591–595.
51. J. Zeng and Z. Guo, *Colloids Surf., A*, 2014, **444**, 283–288.
52. P. C. Chen and Z. K. Xu, *Sci. Rep.*, 2013, **3**, 2776.
53. Y. Wang, S. Tao and Y. An, *J. Mater. Chem. A*, 2013, **1**, 1701–1708.
54. M. Khemakhem, S. Khemakhem and R. Ben Amar, *Colloids Surf., A*, 2013, **436**, 402–407.
55. M. Huang, Y. Si, X. Tang, Z. Zhu, B. Ding, L. Liu, G. Zheng, W. Luo and J. Yu, *J. Mater. Chem. A*, 2013, **1**, 14071–14074.

56. J. Gu, P. Xiao, J. Chen, F. Liu, Y. Huang, G. Li, J. Zhang and T. Chen, *J. Mater. Chem. A*, 2014, **2**, 15268–15272.
57. J. Gu, P. Xiao, J. Chen, J. Zhang, Y. Huang and T. Chen, *ACS Appl. Mater. Interfaces*, 2014, **6**, 16204–16209.
58. (a) L. Tie, Z. Guo and W. Li, *J. Colloid Interface Sci.*, 2014, **436C**, 19–28; (b) L. Tie, Z. Guo and W. Li, *RSC Adv.*, 2014, **5**, 8446–8454.
59. L. Tie, Z. Guo and W. Liu, *J. Colloid Interface Sci.*, 2015, **453**, 142–150.
60. Y. C. Jung and B. Bhushan, *Langmuir*, 2009, **25**, 14165–14173.
61. B. Wang, W. Liang, Z. Guo and W. Liu, *Chem. Soc. Rev.*, 2015, **44**, 336–361.
62. Y. Si and Z. Guo, *Chem. Lett.*, 2015, **44**, 874–883.
63. Z. Shi, W. Zhang, F. Zhang, X. Liu, D. Wang, J. Jin and L. Jiang, *Adv. Mater.*, 2013, **25**, 2422–2427.
64. B. R. Solomon, N. Hyder and K. K. Varanasi, *Sci. Rep.*, 2014, **4**, 5504.